SANICLAY-T: simple thermodynamic-based anisotropic plasticity model for clays

Fabio Rollo [(1)], Angelo Amorosi [(1) *]

(1) Sapienza Università di Roma, Department of Structural and Geotechnical Engineering, via Eudossiana 18, 00184 Roma, Italy (phone: +39-06-44585982, e-mail: angelo.amorosi@uniroma1.it).

* Corresponding Author

Abstract

In this work the anisotropic model for clays SANICLAY proposed by Dafalias & Taiebat (2013) is reformulated within the framework of hyper-elastoplasticity. The model, called SANICLAY-T, is fully defined by two scalar potential functions, the free energy and the rate of dissipation. It is first presented in the triaxial space and then generalised in the multiaxial one. The model reproduces exactly the original one for the case of associate flow rule, while leads to a different outcome for non-associated flow. When compared to existing hyperplastic models accounting for rotational hardening, the proposed one proves to be more versatile, as characterised by less restrictive constraints on the hardening and asymptotic behaviour of the soil. The predictive capability of the model is illustrated with reference to experimental data on natural and reconstituted clays, highlighting its merits and limitations.

Keywords: constitutive modelling, thermodynamics, plasticity anisotropy, clays

1 Introduction

The internal structure of natural soils is rarely isotropic, due to the specific arrangement and orientation of the particles developed during the processes of deposition, consolidation and the subsequent stress/strain history. This leads to an anisotropic character at the macroscopic level, affecting the full range of the mechanical behaviour of soils, that can play a relevant role in many geotechnical engineering problems (e.g. Simpson *et al*., 1996; Zdravković *et al*., 2002; Franzius *et al*., 2005; Karstunen *et al*., 2005; Puzrin *et al*., 2012; Zymnis *et al*., 2013; Cudny & Partyka, 2017; Rezania *et al*., 2017; Simpson, 2017; Sivasithamparam & Rezania, 2017; Rezania *et al*., 2018).

In soil constitutive modelling, anisotropy is often accounted for by mathematical entities, named fabric tensors, that account at the continuum level for the directional character of the internal soil structure. Recent numerical experiments, carried out by the Distinct Element Method (DEM), have clearly indicated that anisotropy affects the whole range of the mechanical behaviour of the investigated ideal granular materials, from the early reversible stage up to the critical state conditions (e.g. Masson & Martinez, 2001; Fu & Dafalias, 2011; Guo & Zhao, 2013; Wang *et al*., 2017; Yang & Wu, 2017; Theocharis *et al*., 2019; Wang *et al*., 2020).

In clays, the anisotropic behaviour often observed in laboratory testing appears intimately related to the corresponding distorted yield surfaces. This has been observed experimentally on various clayey soils by carefully probing undisturbed specimens, retrieved from their natural deposit, in a stress-controlled triaxial system (e.g. Diaz-Rodriguez *et al*., 1992; Smith *et al*., 1992; Callisto & Calabresi, 1998; Chin *et al*., 2007; Huang *et al*., 2011; Kim & Finno, 2012; Liu *et al*., 2013; Al-Sharrad *et al*., 2017). These results suggest that the plastic anisotropic behaviour of clays can be efficiently modelled by a distorted yield surface, inclined with respect to the isotropic axis as originally proposed by Hashiguchi (1977) and Sekiguchi & Ohta (1977), characterised by an evolution law that modifies its degree of distortion according to the direction of the applied stress-strain paths, i.e. accounting for plastic strain induced anisotropy, as suggested by Gens (1982). More recently, within the framework of hardening plasticity, many authors presented constitutive models characterised by distorted and oriented yield surfaces (e.g. Dafalias, 1986; Whittle & Kavvadas, 1994; Wheeler *et al*., 2003; Jiang & Ling, 2010; Dafalias & Taiebat, 2013, 2014; Yang *et al*., 2015; Sivasithamparam & Castro, 2016) in which the evolution of anisotropy is controlled by the so-called "rotational hardening" laws. As a matter of fact, the yield surface is distorted and the result is an apparent rotation around the origin of the stress space according to a specific hardening law: this is why the term "rotational hardening" often denotes this class of elasto-plastic constitutive models. The

directional character of the yield locus in the stress space is described by a tensor-like internal variable that becomes a scalar-valued stress ratio entity under triaxial conditions, for which several evolution laws have been proposed (Zhang *et al.*, 2016).

However, it is well-known that the thermodynamic consistency of the above formulations is not automatically satisfied. Models that violate the thermodynamics principles might lead to unrealistic phenomena, one of which is the absence of dissipation or, even worse, the creation of energy under cyclic loading (Ko & Masson, 1976; Zytynski *et al.*, 1978).

A possible strategy to formulate thermodynamic-based constitutive relationships makes use of internal variables to describe the past history of the material. In this context, it is worth mentioning the hyperplasticity theory proposed by Houlsby & Puzrin (2000, 2006), which can describe a wide range of engineering materials, among which soils, including those exhibiting non-associated plastic flow rules. Basically, it requires the definition of two scalar functions, the free energy and the rate of dissipation.

In light of this, several single-surface hyperplastic models for clays have been developed in the past few years, mainly inspired by the Cam clay-family models (e.g. Collins & Houlsby, 1997; Collins & Kelly, 2002; Einav & Puzrin, 2004b; Coombs & Crouch, 2011; Zhang *et al.*, 2018). To account for plastic anisotropy, Collins & Hilder (2002) introduced a stress-dependent dissipation function which describes a class of distorted yield surfaces, whose shape in the stress space is related to the assumed non-associated flow rule. Along this track, Coombs (2011), Coombs *et al.* (2013) and Coombs (2017) extended the formulation to non-axial symmetric triaxial cases, focusing on the uniqueness of critical state conditions, while Chen & Yang (2019) discussed the role of the rotational hardening laws from a thermodynamic perspective.

The aim of this work is to formulate a single-surface hyperelasto-plastic anisotropic model for clays based on that proposed by Dafalias & Taiebat (2013) within the family of simple anisotropic clay plasticity models SANICLAY (Dafalias *et al.*, 2006). This model has been selected as its mathematical formulation is relatively simple and its performance is realistic enough when compared to experimental observations. The reasons for this reformulation are more than one. First of all, a thermodynamically consistent model called SANICLAY-T will be obtained for both elastic and plastic regimes. Secondly, we show that some of the limitations of the few similar hyperplastic models proposed in the literature can be prevented removing the stored term in the free energy function, once a new expression for the rate of dissipation is provided. Therefore, the SANICLAY-T model admits volumetric isotropic hardening law as in the original SANICLAY one, also allowing the critical state to be anisotropic. Furthermore, a non-associated flow rule will be introduced along the line tracked by Collins & Hilder (2002), leading to a modification of the shape of the yield locus in the Cauchy

stress space as compared to the original distorted ellipse. This aspect plays a crucial role when reproducing the behaviour of frictional materials and significantly improves the predictive capability of the model.

The structure of the paper is as follows. In section 2 the main ingredients of the hyperplastic approach are summarised whereas section 3 is devoted to the description of the SANICLAY-T model. The model is presented in its triaxial formulation first, for both associated and non-associated flow rules, to then discuss its generalisation to the multiaxial stress space. In section 4 the predictive capability of the model is illustrated with reference to experimental results on natural and reconstituted clays.

In the following the soil mechanics sign convention (compressive positive) is assumed, and all stresses are effective stresses. Second order tensors are expressed by subscript notation, where summation is denoted by the repeated indexes. The strain tensor $\varepsilon_{ij} = 1/3\,\varepsilon_{kk}\delta_{ij} + \varepsilon'_{ij}$ and the effective stress $\sigma_{ij} = 1/3\,\sigma_{kk}\delta_{ij} + \sigma'_{ij}$ are symmetric, with the prime denoting their deviatoric parts and δ_{ij} being the Kronecker delta. The stress invariants employed here are the mean effective pressure $p = 1/3\,\sigma_{ii}$ and the deviatoric stress $q = \sqrt{3/2\,\sigma'_{ij}\sigma'_{ji}}$ while the corresponding strain invariants are the volumetric strain $\varepsilon_v = \varepsilon_{ii}$ and the deviatoric strain $\varepsilon_s = \sqrt{2/3\,\varepsilon'_{ij}\varepsilon'_{ji}}$.

2   Thermodynamic constitutive framework

In this section the key ingredients of the hyperplastic approach are briefly summarised. This framework shares many common aspects with the pioneering thermodynamic-based plasticity one discussed in Halphen & Nguyen (1975) and Maugin (1992), then applied to geomaterials by Collins & Houlsby (1997). For a more complete discussion on the hyperplastic framework, the reader should refer to Houlsby & Puzrin (2006).

Basically, two potentials are necessary to define the constitutive behaviour: the free energy function and the dissipation or the yield function, being these latter related each other by a singular Legendre transform. In this study attention is limited to the case of rate independent materials and isothermal processes, hence the energy function is conveniently expressed in terms of the Helmholtz and the Gibbs energies, as the temperature is an independent variable. The use of the Legendre transform allows to switch from one to another form of these functions to formulate the constitutive model in the most convenient way for the specific application. The energy functions depend on the

current stress/strain state and on a series of tensor-like internal variables denoted as α_{ij}. For the purposes of this study, a single tensor variable is considered, though the generalisation to more variables is straightforward, while the thermal effects are neglected. The rate of dissipation function depends on the current state of the material as well as on the rate of the internal variable $\dot{\alpha}_{ij}$ and must be non-negative not to violate the second law of thermodynamics. From the energy and the dissipation functions the generalised stresses $\bar{\chi}_{ij}$ and the dissipative generalised stresses χ_{ij} are defined, as reported in Table 1.

	Gibbs free energy	Helmholtz free energy
Energy function	$\psi = \psi\left(\sigma_{ij},\alpha_{ij}\right)$	$\varphi = \varphi\left(\varepsilon_{ij},\alpha_{ij}\right)$
Stress/strain	$\varepsilon_{ij} = -\dfrac{\partial \psi}{\partial \sigma_{ij}}$	$\sigma_{ij} = \dfrac{\partial \varphi}{\partial \varepsilon_{ij}}$
Generalised stress	$\bar{\chi}_{ij} = -\dfrac{\partial \psi}{\partial \alpha_{ij}}$	$\bar{\chi}_{ij} = -\dfrac{\partial \varphi}{\partial \alpha_{ij}}$
Rate of dissipation	$\dot{d} = \dot{d}^{\psi}\left(\sigma_{ij},\alpha_{ij},\dot{\alpha}_{ij}\right) \geq 0$	$\dot{d} = \dot{d}^{\varphi}\left(\varepsilon_{ij},\alpha_{ij},\dot{\alpha}_{ij}\right) \geq 0$
Dissipative generalised stress	$\chi_{ij} = \dfrac{\partial \dot{d}^{\psi}}{\partial \dot{\alpha}_{ij}}$	$\chi_{ij} = \dfrac{\partial \dot{d}^{\varphi}}{\partial \dot{\alpha}_{ij}}$
Yield function	$f = f^{\psi}\left(\sigma_{ij},\alpha_{ij},\chi_{ij}\right) = 0$	$f = f^{\varphi}\left(\varepsilon_{ij},\alpha_{ij},\chi_{ij}\right) = 0$
Flow rule	$\dot{\alpha}_{ij} = L\dfrac{\partial f^{\psi}}{\partial \chi_{ij}}$	$\dot{\alpha}_{ij} = L\dfrac{\partial f^{\varphi}}{\partial \chi_{ij}}$

Table 1. General formulation for hyperplasticity theory

Under the hypothesis of rate independent material the rate of dissipation is a homogeneous first order function of $\dot{\alpha}_{ij}$ and a degenerate Legendre transform can be identified, providing the yield function *f* and the flow rule in the dissipative generalised stress space, with *L* a non-negative scalar representing the plastic multiplier. Therefore, the formulation is basically defined in the generalised stress space, where the flow rule is by definition associated.

In the following, discussion will be restricted to the stress-based formulation, thus the Gibbs free energy will be conveniently employed. We consider the case of an uncoupled material, for which the Gibbs free energy can be written in the special form (Collins & Houlsby, 1997):

$$\psi = \psi_1\left(\sigma_{ij}\right) - \sigma_{ij}\alpha_{ij} + \psi_2\left(\alpha_{ij}\right) \tag{1}$$

where the term ψ_1 represents the elastic energy function of the stress and ψ_2 is the stored energy depending on the internal variables. Differentiating Eq. (1) with respect to the stress results in the following expression for the total strain:

$$\varepsilon_{ij} = -\frac{\partial \psi}{\partial \sigma_{ij}} = -\frac{\partial \psi_1}{\partial \sigma_{ij}} + \alpha_{ij} = \varepsilon_{ij}^e + \varepsilon_{ij}^p \qquad (2)$$

By virtue of the additive decomposition of the strain in an elastic and plastic parts denoted with the superscripts e and p, respectively, one can ascribe the internal variable α_{ij} to the plastic strain tensor. Furthermore, stemming from the definition of the generalised stress in Table 1, it results:

$$\overline{\chi}_{ij} = \sigma_{ij} - \frac{\partial \psi_2}{\partial \alpha_{ij}} \qquad (3)$$

which provides the link between the stress and the generalised stress. By virtue of the fundamental assumption of the Ziegler's orthogonality principle (Ziegler, 1977), the dissipative generalised stresses and the generalised stresses coincide. Hence, Eq. (3) allows to switch from the yield surface f expressed in terms of χ_{ij} to its dual function $\hat{f}$ in terms of Cauchy stresses and, similarly, to reformulate the flow rule in both generalised and Cauchy stress spaces. The term $\partial \psi_2 / \partial \alpha_{ij}$ is called "back stress" and plays the role of a shift of the yield locus in the σ_{ij} representation as compared to that obtained in the χ_{ij} space. It also introduces a kinematic hardening, as the resulting back stress depends on the internal variable α_{ij}, thus controlling the evolution of the centre of the yield surface without any change in its shape and size. On the other hand, the dependence of the dissipation rate on the internal variables introduces other forms of hardening such as isotropic ones, leading to contraction and expansion of the yield locus with plastic straining. Therefore, mixed kinematic and isotropic hardening is basically obtained by employing the form of the Gibbs free energy of Eq. (1) and introducing a dependence of the dissipation function on the plastic strains. However, it is worth noting that in some cases different combinations of free energy and dissipation functions can lead to the same constitutive model, as discussed by Collins & Houlsby (1997) with reference to the modified Cam clay model: in fact, one can neglect the term ψ_2 in Eq. (1) provided the corresponding additional term $\dfrac{\partial \psi_2}{\partial \alpha_{ij}} \dot{\alpha}_{ij}$ is added in the rate of dissipation, thus guaranteeing that the two formulations are characterised by the same value of the total energy, sum of the elastic, stored and dissipated contributions.

Finally, the dissipation function controls the associative or non-associative character of the flow rule: the irreversible behaviour is by definition associated in the generalised stress space but it becomes non-associated in the Cauchy stress space when the rate of dissipation depends explicitly on σ_{ij}. In such circumstances, the shape of the yield surface in the stress space results as modified if compared to its dual representation in the χ_{ij} space.

3 Thermodynamic-based formulation

In this section the SANICLAY-T model is presented within the framework of hyperelasto-plasticity. The model is first described in triaxial formulation, then the generalisation to the stress-strain space is illustrated.

To guarantee the thermodynamic consistency of the model within the elastic regime, the hypoelastic formulation commonly adopted for this class of elasto-plastic constitutive relationships is substituted by the nonlinear isotropic hyperelastic one by Houlsby *et al*. (2005), leading to the following expression for the Gibbs free energy:

$$
\begin{aligned}
\psi\left(p,q,\alpha_p,\alpha_q\right) &= \psi_1\left(p,q\right)-\left(p\alpha_p+q\alpha_q\right)= \\
&= -\frac{1}{p_r^{1-n}k\left(1-n\right)\left(2-n\right)}\left[p^2+\frac{k\left(1-n\right)}{3g}q^2\right]^{\frac{2-n}{2}}-\left(p\alpha_p+q\alpha_q\right)
\end{aligned}
\tag{4}
$$

where p_r denotes the reference pressure and n, k and g are elastic parameters. Differentiating Eq. (4) with respect to the stress results in the volumetric and deviatoric strains, with the internal variables α_p and α_q representing the volumetric and deviatoric plastic strains, respectively:

$$
\varepsilon_v = -\frac{\partial\psi}{\partial p} = \varepsilon_v^e+\varepsilon_v^p = \frac{1}{p_r^{1-n}k\left(1-n\right)}\left[p^2+\frac{k\left(1-n\right)}{3g}q^2\right]^{-\frac{n}{2}}p+\alpha_p
$$

$$
\varepsilon_s = -\frac{\partial\psi}{\partial q} = \varepsilon_s^e+\varepsilon_s^p = \frac{1}{p_r^{1-n}}\left[p^2+\frac{k\left(1-n\right)}{3g}q^2\right]^{-\frac{n}{2}}\frac{q}{3g}+\alpha_q
\tag{5a,b}
$$

The derivatives of Eq. (4) with respect to the internal variable α_p and α_q provide the generalised stress $\overline{\chi}_p$ and $\overline{\chi}_q$, equal to the stress p and q, respectively, as the stored energy term ψ_2 is null and no elasto-plastic coupling is considered in this work (i.e. the elastic free energy ψ_1 does not depend on plastic strains).

The additional key ingredient to develop the model within the thermodynamic framework is the dissipation function, specifically chosen to re-obtain the yield surface originally proposed by Dafalias (1986). First, the case of associated flow rule is discussed and then the model is generalised to account for non-associated plasticity.

3.1 Associated flow rule

The rate of dissipation is defined as:

$$\dot{d}\left(\dot{\alpha}_p,\dot{\alpha}_q,\beta,p_0\right)=\frac{p_0}{2}\left[\sqrt{\left(\dot{\alpha}_p+\beta\dot{\alpha}_q\right)^2+\left(M^2-\beta^2\right)\dot{\alpha}_q^2}+\dot{\alpha}_p+\beta\dot{\alpha}_q\right] \tag{6}$$

where M denotes the slope of the critical state line in the p-q plane, the internal variable p_0 is the preconsolidation pressure and the non-dimensional internal variable β is a stress ratio-like scalar value that controls the plastic anisotropy of the material (we denote here the internal variable with β instead of α as in Dafalias & Taiebat (2013) as the latter refer to the generic internal variable of the hyperplastic framework).

In combination with Eq. (6), two hardening laws are introduced. The first one is a volumetric isotropic hardening governing the contraction and the expansion of the elastic domain via the internal variable p_0, whose evolution is controlled by the volumetric plastic strain rate according to the well-known relation:

$$\dot{p}_0=\frac{1+e_{in}}{\lambda-\kappa}p_0\dot{\alpha}_p \quad \Rightarrow \quad p_0=p_{0,in}\exp\left(\frac{1+e_{in}}{\lambda-\kappa}\alpha_p\right) \tag{7}$$

where λ and κ are the slope of the normal consolidation line and the swelling line in the e-ln$p$ plane, respectively, and e_{in} and $p_{0,in}$ are the initial void ratio and preconsolidation pressure.

Secondly, a rotational hardening law expressed as the rate of the internal variable β controls the distortion of the yield locus and its evolution with plastic strain. Several rotational hardening laws are available in the literature and, even for the SANICLAY model, different rules have been proposed in last few years. In this study, for reasons discussed in Dafalias *et al*. (2020), we adopt the following rate evolution equation:

$$\dot{\beta}=\langle L\rangle cp\left(\beta_b-\beta\right) \tag{8}$$

where c is a model parameter controlling the pace of the evolution and β_b represents the equilibrium "bounding" value, function of the current stress ratio η. Along a fixed η stress path the surface rotates from the initial configuration until reaching and then maintaining the equilibrium

position, while continues to harden isotropically. Here we adopt the simplest expression, among those proposed in the literature, for the equilibrium (bounding) value of β: $\beta_b(\eta) = \eta/x$, with x being a model parameter (Dafalias, 1986). Nevertheless, alternative expressions aimed at limiting excessive rotations of the yield surface and at controlling the anisotropy at critical state are possible. To this purpose, the law discussed by Dafalias & Taiebat (2014) is recalled:

$$\beta_b = \eta \left\{ \frac{\beta_c}{M} + m \left[1 - \left(\frac{|\eta|}{M} \right)^{n*} \right] \right\} \quad \text{for} \quad |\eta| < M$$

$$\beta_b = \eta \frac{\beta_c}{M} \exp \left[-\mu \left(\frac{|\eta|}{M} - 1 \right) \right] \quad \text{for} \quad |\eta| > M$$

(9a,b)

where β_c is the value of β for $\eta = M$ and $m, n*, \mu$ are model parameters (note that the asterisk is introduced to avoid confusion with the elastic exponent n of Eq. (4)).

As expected for rate independent materials, the rate of dissipation is a homogeneous first order function of the rates of the internal variables and, according to the hypothesis of associated flow rule, is independent of the stress. Note that as p_0 is a positive quantity, the dissipation function satisfies the condition $\dot{d} \geq 0$ for any value of $\dot{\alpha}_p$ and $\dot{\alpha}_q$ if the condition $|\beta| < M$ is respected: this was already necessary in the SANICLAY model to guarantee a real solution of the yield function but in this case the same condition stems from a thermodynamic requirement. Furthermore, it is worth noting that the only way for which Eq. (6) is zero, apart from the obvious case in which the behaviour is purely elastic, is for $\dot{\alpha}_p < 0$ and $\dot{\alpha}_q = 0$. However, the former case holds for $p = 0$ only, a limiting condition for the class of soils under study which also characterises the original SANICLAY formulation.

Finally, by virtue of the degenerate Legendre transform, the yield surface in the dissipative generalised stress space $\chi_p - \chi_q$ is obtained from the dissipation function. For the sake of conciseness, the analytical procedure to obtain the dual function is reported in Appendix A. The yield surface results in:

$$f(\chi_p, \chi_q, \beta, p_0) = (\chi_q - \beta \chi_p)^2 - (M^2 - \beta^2) \chi_p (p_0 - \chi_p) = 0$$

(10)

Furthermore, the Ziegler's orthogonality principle allows to express Eq. (10) in term of stress, leading to:

$$\hat{f}(p, q, \beta, p_0) = (q - \beta p)^2 - (M^2 - \beta^2) p (p_0 - p) = 0$$

(11)

that is the distorted ellipse proposed by Dafalias (1986), thus demonstrating that, apart from the elastic regime, the associated version of the SANICLAY model is consistent with the laws of thermodynamics. For the special case of $\beta = 0$ the modified Cam clay ellipse is recovered.

3.2 Non-associated flow rule

In principle there are several ways in which the current stress can be enforced in the dissipation function to end up with a non-associated flow rule. Here, along the line tracked by Collins & Hilder (2002), we generalise the rate of dissipation of Eq. (6) as:

$$\dot{d}\left(\dot{\alpha}_p,\dot{\alpha}_q,\beta,p_0,p\right) = \sqrt{A^2\left(\dot{\alpha}_p + \beta\dot{\alpha}_q\right)^2 + B^2\left(M^2 - \beta^2\right)\dot{\alpha}_q^2} + \frac{\gamma p_0}{2}\left(\dot{\alpha}_p + \beta\dot{\alpha}_q\right) \qquad (12)$$

where A and B are stress-like quantities defined as:

$$A = \left(1-\gamma\right)p + \frac{\gamma p_0}{2}; \quad B = \left(1-\delta\right)p + \frac{\gamma\delta p_0}{2} \qquad (13a,b)$$

where γ and δ are two additional dimensionless parameters varying from zero to one. For $\gamma = \delta = 1$ Eq. (12) coincides with Eq. (6) as the terms A and B no longer depend on the mean effective pressure and the case of associated flow rule in the stress space is recovered. Conversely, as A and B generally depend on the stress, the yield function in the p-q plane is no longer an ellipse and, as expected, the flow rule becomes non-associated. Furthermore, depending on the parameters γ and δ the yield surface in the stress space can be locally concave for small stress levels (Collins & Kelly, 2002; Collins, 2003). It is worth noting that Eq. (12) is always strictly positive during plastic loading, even for the case $\dot{\alpha}_p < 0$ and $\dot{\alpha}_q = 0$ being $A > \gamma p_0/2$.

The parameters γ controls the ratio p/p_0 at critical state while δ governs the slope of the tangent to the yield surface corresponding to the critical state condition. As A and B do not depend on the deviatoric stress q, the shape of the yield surface is symmetric in compression and extension (Collins & Hilder, 2002). However, according to Coombs (2017), an alternative procedure could be adopted to obtain non-circular deviatoric sections of the yield surface, introducing a Lode angle dependency in the dissipation function.

The yield function in the dissipative generalised stresses χ_p and χ_q is derived from Eq. (12), as illustrated in detail in Appendix A, analogously to what done for the associated case. It results in:

$$f\left(\chi_p,\chi_q,\beta,p_0,p\right) = A^2\left(\chi_q - \beta\chi_p\right)^2 + B^2\left(M^2 - \beta^2\right)\left(\chi_p - \frac{\gamma p_0}{2}\right)^2 - A^2 B^2\left(M^2 - \beta^2\right) = 0 \quad (14)$$

The yield locus of Eq. (14) is a distorted ellipse in the χ_p - χ_q plane with centre lying on the line of slope β, as shown in Figure 1. The position of the centre C of the ellipse, with coordinates $(\gamma p_0/2, \gamma\beta p_0/2)$ depends on the parameters γ while the terms A and B control the size of the yield locus. The points D and E in Figure 1 have coordinates $((\gamma-1)p, \beta(\gamma-1)p)$ and $((1-\gamma)p+\gamma p_0, \beta(1-\gamma)p+\beta\gamma p_0)$, respectively. Therefore, the yield surface passes through the origin of the χ_p - χ_q axes only for the case $\gamma = 1$. In other words, the size and the position of the ellipse in the dissipative generalised stress plane depend on the parameters γ and δ and on the current values of p and p_0.
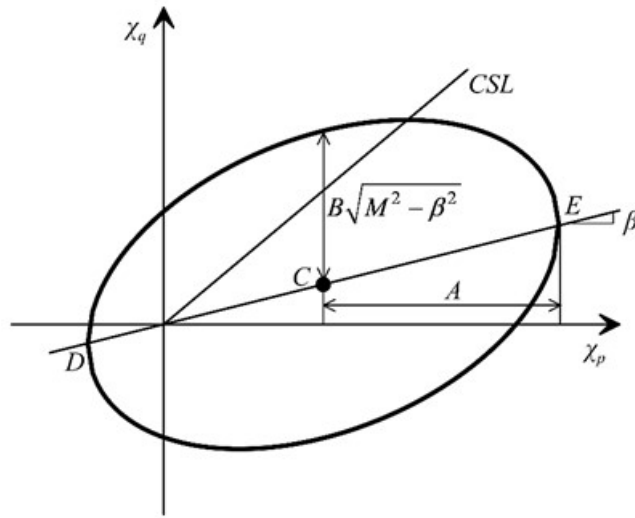

Figure 1. Yield surface in the dissipative generalised stress space

Again, recalling the orthogonality condition and that the generalised stresses $\overline{\chi}_p$ and $\overline{\chi}_q$ coincide with the mean pressure p and the deviatoric stress q, respectively, as no back stresses are expected, one can write the new yield function in terms of the stress:

$$\hat{f}(p,q,\beta,p_0) = A^2(q-\beta p)^2 + B^2(M^2-\beta^2)\left(p-\frac{\gamma p_0}{2}\right)^2 - A^2 B^2(M^2-\beta^2) = 0 \tag{15}$$

Although Eqs. (14) - (15) are analogous from an analytical perspective, their representations in the dissipative generalised and Cauchy stress spaces are different as A and B depend on the current value of p. Eq. (14) is a distorted ellipse in the χ_p - χ_q plane while Eq. (15) assumes different shapes in the p-q plane depending on the parameters γ and δ. In fact, within the framework of hyperplasticity, the modification of the dissipation function by the introduction of a dependence on the mean effective pressure leads to a yield surface in the stress space that is no longer an ellipse.

As a consequence, there is no way to reproduce the original non-associated model proposed by Dafalias & Taiebat (2013) by the procedure adopted here. In fact, in the traditional elasto-plastic formulation both yield and plastic potential surfaces are distorted ellipses, with the constant N substituting for M in the expression of the yield surface. What above does not necessarily mean that the non-associated version of the original SANICLAY model is thermodynamically inconsistent, but rather that the rigorous approach adopted here, despite its well-recognized advantages, does not allow to choose the yield function and the flow rule independently of each other, as typically done in classical elastoplasticity. Nevertheless, while the proposed formulation is by definition always thermodynamically consistent, this is not a priori true for the non-associated Dafalias & Taiebat (2013) model, for which the non-negativeness of the dissipation has to be guaranteed along any loading process by a proper choice of the model parameters. Furthermore, it is worth noting that within the procedure adopted here, the determination of the plastic potential function would be an unnecessary mathematical complication as the flow rule stems directly from the derivatives of Eq. (14) with respect to the generalised stresses.

For completeness, all the derivatives of the hyperplastic model, necessary to reformulate it in incremental form, are summarised in Appendix B.

3.3 Multiaxial formulation

The SANICLAY-T model can be straightforwardly generalised to the multiaxial stress-strain space. The Gibbs free energy of Eq. (4) now assumes the form:

$$\psi\left(\sigma_{ij}, \alpha_{ij}\right) = \psi_1\left(\sigma_{ij}\right) - \sigma_{ij}\alpha_{ij} =$$

$$= -\frac{1}{p_r^{1-n}k(1-n)(2-n)}\left[\left(\frac{1}{9} - \frac{k(1-n)}{6g}\right)\left(\sigma_{ii}\right)^2 + \frac{k(1-n)}{2g}\sigma_{ij}\sigma_{ij}\right]^{\frac{2-n}{2}} - \sigma_{ij}\alpha_{ij} \tag{16}$$

where the tensor-like internal variable α_{ij} represents the plastic strain tensor.

The dissipation function for the general case of non-associated plasticity is expressed in the following form, adopting for the internal variable α_{ij} the decomposition in its isotropic and deviatoric parts $\alpha_{ij} = \frac{1}{3}\alpha_p\delta_{ij} + \alpha'_{ij}$ and expressing the tensor value rotational variable β_{ij} such that its triaxial counterpart is $\beta = \sqrt{3/2\,\beta_{ij}\beta_{ij}}$:

$$d\left(\dot{\alpha}_{ij}, \beta_{ij}, p_0, p\right) = \sqrt{A^2\left(\dot{\alpha}_p + \beta_{ij}\dot{\alpha}'_{ij}\right)^2 + B^2\left(M^2 - \frac{3}{2}\beta_{kl}\beta_{kl}\right)\frac{2}{3}\dot{\alpha}'_{ij}\dot{\alpha}'_{ij}} + \frac{\gamma p_0}{2}\left(\dot{\alpha}_p + \beta_{ij}\dot{\alpha}'_{ij}\right) \tag{17}$$

with M possibly depending on the Lode angle. Analogously to what previously illustrated, the singular Legendre transform provides the yield surface in the dissipative generalised stress space:

$$f\left(\chi_{ij},\beta_{ij},p_0,p\right)=A^2\left(\chi'_{ij}-\beta_{ij}\chi_p\right)\left(\chi'_{ij}-\beta_{ij}\chi_p\right)+B^2\left(M^2-\frac{3}{2}\beta_{ij}\beta_{ij}\right)\left(\chi_p-\frac{\gamma p_0}{2}\right)^2+$$
$$-A^2B^2\left(M^2-\frac{3}{2}\beta_{ij}\beta_{ij}\right)=0 \tag{18}$$

where the dissipative generalised stress tensor is decomposed in its isotropic and deviatoric parts $\chi_{ij}=\chi_p\delta_{ij}+\chi'_{ij}$. For the Ziegler's orthogonality principle, the yield surface in the general stress space becomes:

$$\hat{f}\left(\sigma_{ij},\beta_{ij},p_0\right)=\frac{3}{2}A^2\left(\sigma'_{ij}-\beta_{ij}p\right)\left(\sigma'_{ij}-\beta_{ij}p\right)+B^2\left(M^2-\frac{3}{2}\beta_{ij}\beta_{ij}\right)\left(p-\frac{\gamma p_0}{2}\right)^2+$$
$$-A^2B^2\left(M^2-\frac{3}{2}\beta_{ij}\beta_{ij}\right)=0 \tag{19}$$

Finally, the rotational hardening rule of Eq. (8) generalises into:

$$\dot{\beta}_{ij}=\langle L\rangle cp\left(\beta_{b,ij}-\beta_{ij}\right) \tag{20}$$

Where, according to Dafalias & Taiebat (2013, 2014), in the expressions of the equilibrium "bounding" value the stress ratio η is substituted by the stress ratio tensor $r_{ij}=\sigma'_{ij}/p$ and of $|\eta|$ by $\sqrt{3/2\,r_{ij}r_{ij}}$.

3.4 Discussion on the proposed formulation

In this section the proposed formulation is discussed and compared to existing ones, aiming at highlighting its possible advantages and limitations.

As a first premise it is worth recalling that, in general, different combinations of Gibbs free energy and rate of dissipation functions can lead to similar constitutive outcomes, as discussed in Collins & Houlsby (1997) and Houlsby & Puzrin (2006). In particular, one option is that of including the term ψ_2, which brings in a back stress controlling the position of the yield locus in the stress space during the loading process, thus explicitly introducing a form of kinematic hardening via the energy function. Alternatively, as in this study, this term can be neglected, i.e. $\psi_2=0$, while adding an integrable term in the rate of dissipation which accounts for the current values of the isotropic and rotational hardening internal variables, that in Eqs. (6) and (12) takes the form $\frac{p_0}{2}\left(\dot{\alpha}_p+\beta\dot{\alpha}_q\right)$. Houlsby (2019) provides an effective geometric interpretation of the above choices with reference to the Modified

Cam-Clay model: in the first case ($\psi_2 \neq 0$) the formulation implies an isotropic expansion of the yield surface about its centre coupled with a translation of the centre (kinematic hardening), while the second option ($\psi_2 = 0$) does not involve the translation, as it assumes that the focus for the isotropic expansion of the yield surface is not the centre of the ellipse but the origin of the stress space. For simple volumetric isotropic hardening models, as the Modified Cam-Clay, the two different options lead to the same incremental formulation while this is not necessarily true for models including more complex hardening forms, as those discussed in this paper.

The proposed formulation has much in common with the anisotropic models discussed in Collins & Hilder (2002) and Coombs (2017) within the framework of hyperplasticity, though differs from those models for the specific forms of the free energy and rate of dissipation, in the sense discussed above. In fact, in the above mentioned models the yield surface in the generalised stress space is a distorted ellipse centred in the axes origin: this introduces the need for back mean normal and deviatoric stresses to obtain the desired representation of the yield surface in the Cauchy stress space. Therefore, with reference to the Gibbs free energy of Eq. (1), both formulations account for a similar stored energy term ψ_2 which, for instance, according to Collins & Hilder (2002) assumes the form:

$$\psi_2 = \left(\tilde{\lambda} - \tilde{\kappa} \right) \frac{\gamma p_0}{2} = \left(\tilde{\lambda} - \tilde{\kappa} \right) \frac{\gamma p_{0,in}}{2} \exp \left(\frac{\alpha_p + \beta \alpha_q}{\tilde{\lambda} - \tilde{\kappa}} \right) \tag{21}$$

where $\tilde{\lambda}$ and $\tilde{\kappa}$ are the slopes of the virgin and the swelling lines in the $\ln p - \ln v$ plane such that the centre of the yield surface in the stress space is $\left(\gamma p_0 / 2, \beta \gamma p_0 / 2 \right)$. The presence of the stored energy of Eq. (21) implies two relevant consequences: (i) the isotropic hardening variable p_0 depends on both volumetric and deviatoric plastic strains and (ii) the free energy continues to accumulate at critical state. Recently, Chen & Yang (2019) claimed that (ii) is a thermodynamically inadmissible result that can be solved by a proper choice of the rotational hardening law characterised by $\beta = 0$ at critical state (i.e. the yield surface is forced to align back to the hydrostatic axis at critical state). We do not share the same opinion, believing that the only thermodynamic requirement that should always hold, thus also at critical state, is the following more general energy balance:

$$\dot{\psi} + \dot{d} = -\varepsilon_{ij} \dot{\sigma}_{ij} \tag{22}$$

which does not imply $\dot{\psi} = 0$: it allows a more general class of anisotropic critical states as compared to those considered by Chen & Yang (2019). In this perspective, the models proposed by Collins & Hilder (2002) and by Coombs (2013, 2017) are thermodynamically consistent and represent key

achievements in modelling anisotropic hardening of clays. The only concern is in the constraints all these formulations imply on the isotropic part of the hardening law, i.e. point (i) of above.

The manipulation of the free energy and the dissipation functions pursued in this work overcomes the above drawbacks. As the stored energy $\psi_2 = 0$, the current value of the internal variable p_0 only enters in the rate of dissipation and the yield function in the stress space is obtained regardless of the adopted isotropic hardening rule. In this sense the present formulation is less restrictive and allows to employ any isotropic hardening law, including those that only depend on the volumetric plastic strains, as often assumed when modelling clayey soils. Furthermore, the thermodynamic consistency of the model at critical state is guaranteed for any value of β, though one can still consider the $\beta = 0$ condition adopting different rotational hardening laws, like those proposed by Dafalias & Taiebat (2014). Therefore, the model can take into account the anisotropic character at critical state, as supported by numerical simulations based on the Discrete Element Method (DEM) (e.g. Wang *et al*., 2017; Yang & Wu, 2017; Theocharis *et al*., 2019; Wang *et al*., 2020), at the same time satisfying the more restrictive requirement $\dot{\psi} = 0$ considered by Chen & Yang (2019).

4   Numerical implementation

The proposed formulation has been implemented in a constitutive driver, to mimic the response of a single Gauss point of a finite element numerical code, adopting an explicit integration scheme. At this scope, the incremental formulation of the model has first been derived (see Appendix B), combining the consistency condition and the flow rule to generate the relationship between stress increments and total strain increments which, by virtue of the additive decomposition of the strain tensor into its elastic and plastic contributions, leads to the following equation:

$$\dot{\sigma}_{ij} = D_{ijkl}^{ep}\dot{\varepsilon}_{kl} = \left(D_{ijkl} - \frac{D_{ijmn}\dfrac{\partial f}{\partial \chi_{mn}}\dfrac{\partial \hat{f}}{\partial \sigma_{pq}}D_{pqkl}}{\dfrac{\partial \hat{f}}{\partial \sigma_{ij}}D_{ijkl}\dfrac{\partial f}{\partial \chi_{kl}} + H} \right)\dot{\varepsilon}_{kl} \tag{23}$$

where D_{ijkl} is the fourth-order elastic stiffness tensor provided by Houlsby *et al*. (2019) as the Legendre transform of the $\psi_1\left(\sigma_{ij}\right)$ term of Eq. 16, and *H* is the hardening modulus, which takes the form:

$$H = -\frac{\partial \hat{f}}{\partial p_0} \frac{1+e_{in}}{\lambda - \kappa} p_0 \frac{\partial f}{\partial \chi_p} - \frac{\partial \hat{f}}{\partial \beta_{ij}} cp\left(\beta_{b,ij} - \beta_{ij}\right) \tag{24}$$

Only the calculation of the first derivatives of the yield surface with respect to the current stress and hardening variables are necessary, as illustrated in detail in Appendix B.

The explicit integration algorithm adopted here requires the yield surface, the hardening laws and the gradient of the plastic flow rule to be evaluated and updated at each calculation step. As customary in explicit schemes, if the final stress lies within the yield domain purely elastic deformations occur and the model response can be calculated exactly, as the hyperelastic formulation is characterised by a one-to-one relationship between stress and strain. Conversely, the solution is approximated by the adopted numerical integration when the yield surface is attained and plastic flow occurs.

It is worth noting that the hyperplastic framework simplifies the integration procedure for the case of non-associated flow rule as compared to the traditional elasto-plastic one. In fact, within this latter approach plastic flow is typically obtained by imposing the plastic potential surface passing through the current stress state, thus requiring the introduction of a dummy scalar variable, controlling the size of the plastic potential surface, which does not have a specific physical meaning. Conversely, for the adopted approach the introduction of such a dummy variable is unnecessary as the plastic flow is directly evaluated as the derivative of the yield surface in the dissipative generalised stress space with respect to χ_{ij}, related to the current stress σ_{ij} through Eq. (3).

5 Response of the model

In this section the response of the anisotropic hyperplastic model is discussed with reference to both the associated and non-associated flow rules. First, the influence of the parameters γ and δ on the flow rule and on the shape of the yield surface in the stress space are presented. Then, the predictive capability of the model is illustrated with reference to some experimental results obtained from laboratory tests on natural and reconstituted clays, highlighting the versatility of the model when accounting for non-associated flow.

Figure 2 depicts the yield surfaces in the normalised plane $p/p_0 - q/p_0$ for fixed rotational variable $\beta = 0.3$, constant $M = 1.08$ and different values of the parameters γ and δ. As expected, only for $\gamma = \delta = 1$ the original distorted ellipse is retrieved. In particular, the case (b) of Figure 2 shows that for $\delta = 0$ (but in general for small values of δ) the yield locus is locally concave near the origin

of the p/p_0 axis and becomes more "tear drop" shaped, while for $\delta = 1$ the surface is unrealistically larger near the origin than in correspondence of $p = p_0$ (Figure 2(c)).
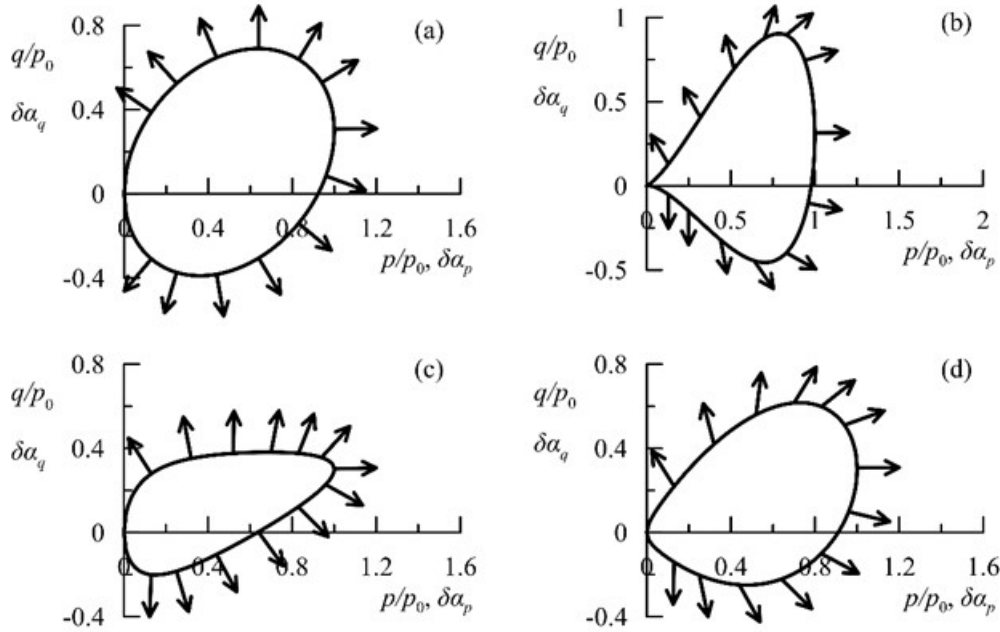

Figure 2. Yield surface in the stress space for (a) $\delta = 1$, $\gamma = 1$, (b) $\delta = 0$, $\gamma = 1$, (c) $\delta = 1$, $\gamma = 0.5$, (d) $\delta = 0.4$, $\gamma = 0.6$

The parameters γ and δ control the non-associativeness of the flow rule in the stress space. Again, the only case in which the flow rule is associated in the p-q plane is when $\gamma = \delta = 1$ whereas the flow rule is, by definition, always associated in the generalised stress space. The arrows in Figure 2 represent the plastic strain rate vectors superposed to the yield surfaces by virtue of the hypothesis of coaxiality between those vectors and the stresses.

It is worth mentioning that the determination of a plastic potential surface, besides the fact that is analytically challenging, is not necessary in the hyperplastic procedure as the plastic strain increments are given by the normal to the yield surface in the generalised stress space, as highlighted by Collins & Hilder (2002). Then, by virtue of the Ziegler's principle, the plastic strain rate is known for any couple of (p, q). This is an advantage from a numerical perspective as no intersection or projection of the current stress state on the plastic potential surface is required to determine the direction of the current plastic strain rate. Nevertheless, one can obtain something similar to a plastic potential surface when representing the dissipative yield surface of Eq. (14) in the p-q plane, as suggested by Collins (2005). In particular, for a fixed value of p/p_0 (and hence for fixed A and B) the dissipative yield surface in the stress space is an ellipse intersecting the yield locus in correspondence of the same value, as depicted in Figure 3. Clearly, the normal to the dissipative ellipse in that point denotes the direction of the plastic strain rate.
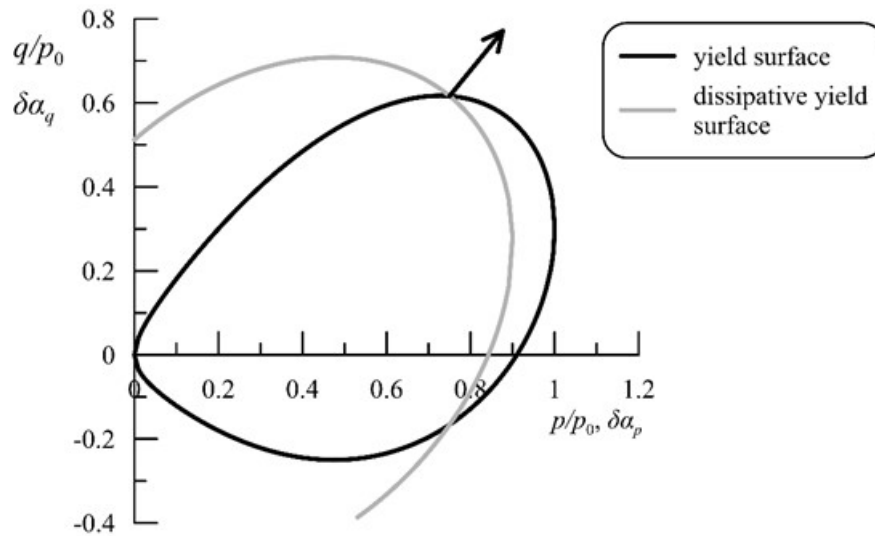
Figure 3. Yield surface and dissipative ellipse in the stress space ($\delta = 0.4$, $\gamma = 0.6$)

The non-associated formulation allows to realistically reproduce the shape of the yield surface in the *p-q* plane experimentally observed on natural clays, by a proper choice of the parameters γ and δ. At this scope, Figure 4 depicts the yield points for the natural Pisa clay (Callisto & Calabresi, 1998) and Taipei clay (Chin *et al.*, 2007) obtained by probing undisturbed samples after reconsolidation to the in situ stress state. In the same figure, the yield surfaces predicted by the model for both associated and non-associated cases are plotted. The values of the internal variable β were determined to fit the experimental data according the values of *M* provided by the Authors. The relevant parameters are summarised in Table 2. Figure 4 shows that the non-associated formulation is more versatile than the associated one as it allows to adapt the shape of the yield surface to the experimental data.
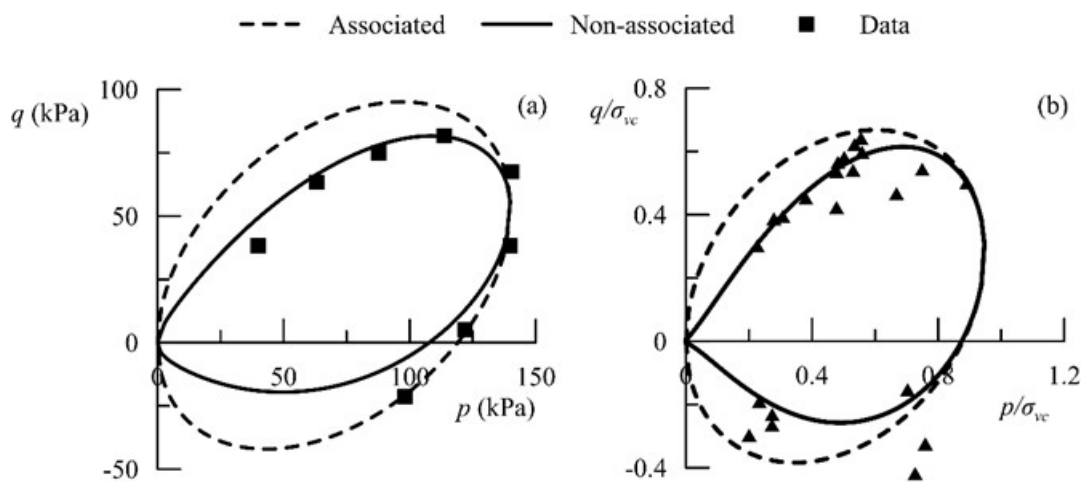

Figure 4. Yield loci for (a) Pisa clay and (b) Taipei clay

Parameter	Values	
	Taipei clay	Pisa clay
M	1.11	0.98
β	0.3	0.38
γ	0.45	0.5
δ	0.1	0.4

Table 2. Yield surface parameters for two natural clays

A list of the model parameters is reported in Table 3. The parameters of SANICLAY-T differ from those of the Dafalias & Taiebat (2013, 2014) models for the elastic constants and for γ and δ controlling the flow rule of the model. The elastic parameters should be calibrated to reproduce the non-linear dependence of the elastic stiffness on the current stress state within the very small strain range, as discussed by Houlsby *et al.* (2005) and, more recently, by Amorosi *et al.* (2020). The reference pressure is assumed by default equal to $p_r = 100\,\text{kPa}$ whereas, in absence of specific laboratory or field investigations, k, g and n can be selected to control the response of the model within the yield surface, recalling that for isotropic stress states $k/g = 2(1+\nu)/\left[3(1-2\nu)\right]$, where ν is the Poisson's ratio. For the constants γ and δ a trial and error procedure can be adopted to reproduce the shape of the yield surface that better fits the experimental results, as shown in Figure 4, and to simulate the behaviour observed in laboratory tests (e.g. triaxial tests) in clays. The remaining parameters coincide with those of Dafalias & Taiebat (2013, 2014): the reader can refer to those papers for detailed discussions on their calibration procedures.

The predictive capability of the model is first illustrated with reference to a series of experimental data obtained by Wheeler *et al.* (2003) on the natural Otaniemi clay. Undisturbed samples were subjected to two loading stages characterised by constant stress ratio η. Samples were first loaded along η_1 to a final mean effective pressure p_{f1}, unloaded along the same path to $p = 5\,\text{kPa}$ and then reloaded following a different stress ratio η_2 to a final mean effective pressure p_{f2}. According to Wheeler *et al.* (2003) the initial inclination and size of the yield surface are $\beta = 0.42$ and $p_0 = 20\,\text{kPa}$. The parameters of the model are summarised in Table 3. The elastic parameter n is close to the unity such that the elastic stiffness depends linearly on the mean effective pressure, as typically assumed in the Cam clay-like models. The constant k is calibrated to reproduce the slope of the rebound line in the $\varepsilon_v - \log p$ plane and g is determined recalling that for isotropic stress states $k/g = 2(1+\nu)/\left[3(1-2\nu)\right]$, where ν is the Poisson's ratio, equal to 0.2 for Otaniemi clay. The parameter x controlling the bounding value β_b under fixed η loading was provided by Dafalias &

Taiebat (2013) while the parameters γ and δ are calibrated to best fit the laboratory results obtained by Wheeler *et al.* (2003).

Parameters	Values	
	Otaniemi clay	LCT clay
p_r	100	100
N	0.99	0.75
K	116.7	239.3
G	70	130
M_c	1.1	1.18
M_e	1.1	0.86
λ	0.44	0.066
κ	0.04	0.0077
γ	0.2 (1.0)	0.55
δ	0.4 (1.0)	0.52
c	20	120
x	1.71	-
β_c	-	0.23
m	-	0.41
n^*	-	9
μ	-	19

Table 3. Model parameters for the tested soils

Figure 5 shows the comparison between the experimental data and the response of the model for both associated ($\gamma = \delta = 1$) and non-associated flow rules. Figures 5(a) and 5(c) prove that the non-associated formulation provides a better prediction of the yield stress during the first loading stage as compared to the associated one, since the yield locus is no longer an ellipse. Furthermore, the corresponding strain paths in Figures 5(b) and 5(d) are well reproduced by the introduction of the non-associated flow rule while in both cases the model underestimates the volumetric strains occurring during the first loading stage of the third test (Figures 5(e) and 5(f)).
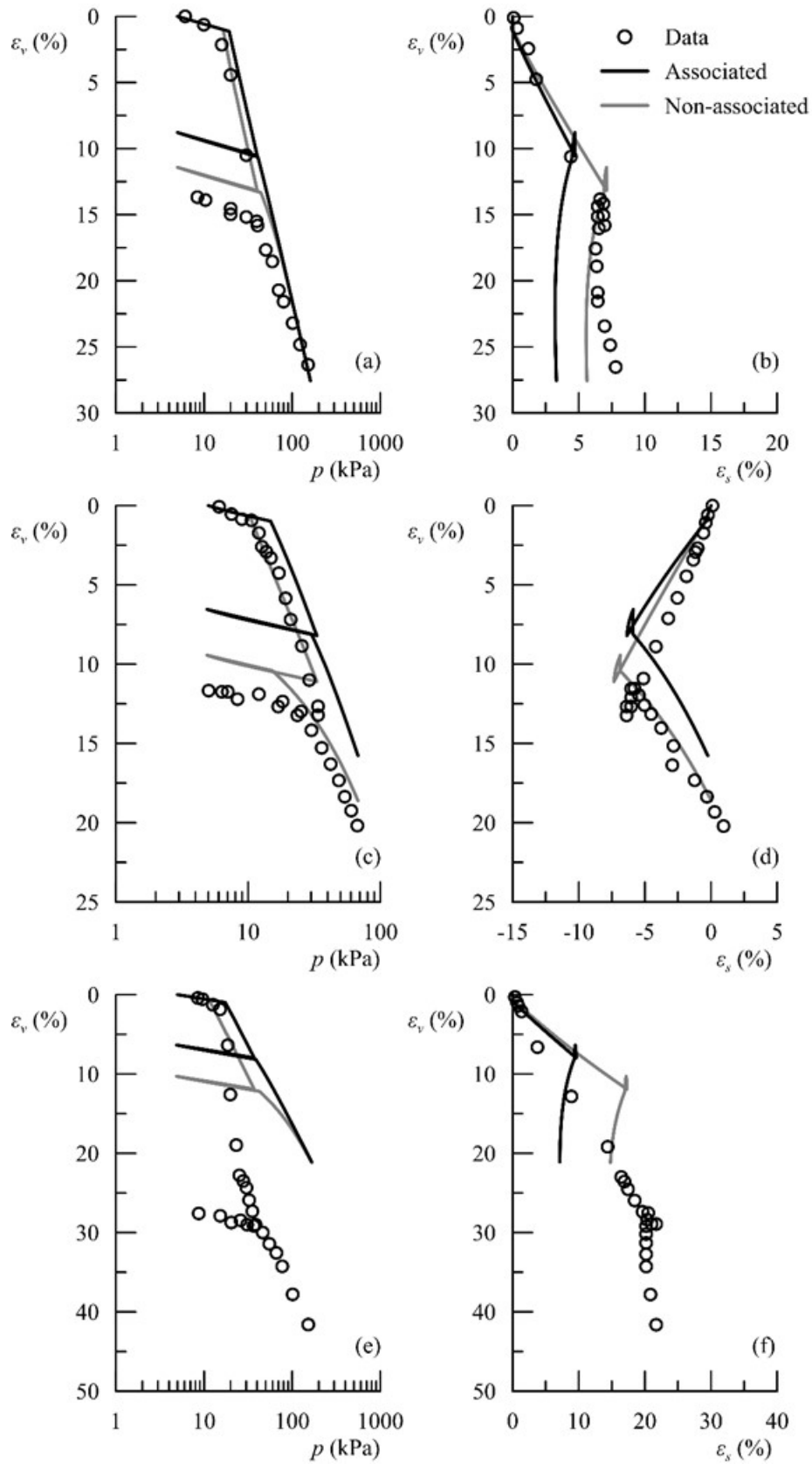
Figure 5. Otaniemi clay: comparison between data and simulations. (a,b) $\eta_1 = 0.6$, $p_{f1} = 40\,\text{kPa}$, $\eta_2 = 0.1$, $p_{f2} = 150\,\text{kPa}$, (c,d) $\eta_1 = -0.59$, $p_{f1} = 33\,\text{kPa}$, $\eta_2 = 0.51$, $p_{f2} = 66\,\text{kPa}$, (e,f) $\eta_1 = 0.9$, $p_{f1} = 37\,\text{kPa}$, $\eta_2 = 0.13$, $p_{f2} = 151\,\text{kPa}$.

The predictive capability of the model is shown in terms of simulations of undrained triaxial tests against experimental data for LCT clay (Gens, 1982). The samples were consolidated under isotropic and anisotropic (K_0) conditions, then unloaded at various OCR and compressed in a triaxial apparatus under undrained conditions. Figure 6 compares the numerical prediction with the experimental data for the one-dimensional K_0 compression and swelling in the p-q plane. The model is characterised by non-associated flow rule and for the equilibrium bounding value β_b the expression of Eq. (9) is adopted to obtain the best back-prediction of the data. The model parameters are synthesised in Table 3. The material is initially isotropic, with $\beta = 0$ and $p_0 = 70\,\text{kPa}$, then subjected to a one-dimensional compressive strain path to a mean effective pressure $p = 233.3\,\text{kPa}$ followed by unloading to $p = 62\,\text{kPa}$. The yield surface of the model undergoes a distortion under compression with a final value of $\beta = 0.4$, whereas the unloading response is purely elastic. The model well reproduces the experimental results.
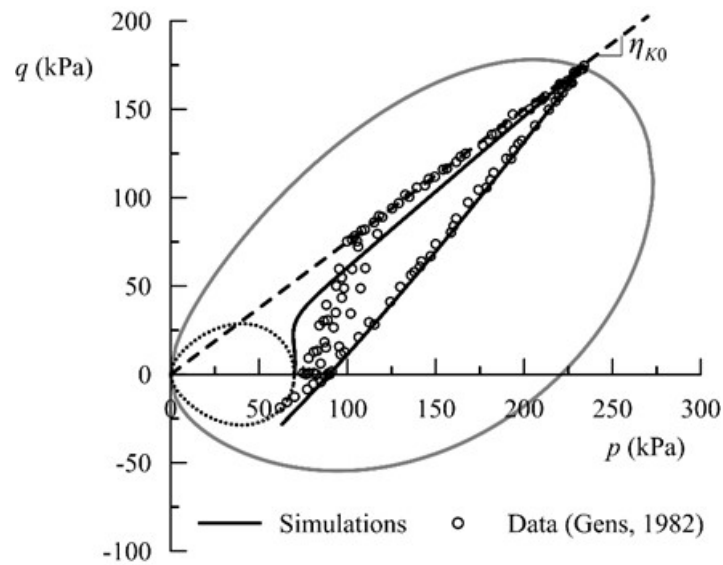

Figure 6. Comparison between data and simulations of one-dimensional consolidation and swelling for LCT clay

Figure 7 shows the behaviour under undrained triaxial compression and extension. The results are plotted in terms of stress paths in the p-q plane and stress-strain curves in the $\varepsilon_s - q$ plane. The samples were reconsolidated at values of OCR = 1, 1.5, 2, 4, 10 for isotropically consolidated states and at OCR = 1, 2, 4, 7 for K_0 consolidated ones. A first observation is that, despite its analytical simplicity, the proposed formulation nicely reproduces the behaviour of samples tested at different stress states and OCR using a single set of constitutive parameters. The overall response of the model is not noticeably different from what predicted by the original non-associated elasto-plastic

formulation (Dafalias & Taiebat, 2014). Nonetheless, it is worth noting that (i) the stress paths of the isotropically consolidated elements (Figure 7(a)) no longer show the hook-type shape close to the critical state which characterised the original elasto-plastic formulation of the model as a consequence of the continuous evolution of the rotational variable at fixed p_0, and (ii) for the anisotropically consolidated tests the non-associated flow rule reproduces softening for normally and slightly overconsolidated samples (Figure 7(c)-(d)). Furthermore, the response in the *p-q* plane is significantly improved by the nonlinear hyperelastic formulation. In fact, the nonlinear dependence of the elastic stiffness on the current stress state produces a volumetric-deviatoric coupling that is responsible of a curvature of the stress paths within the elastic domain.
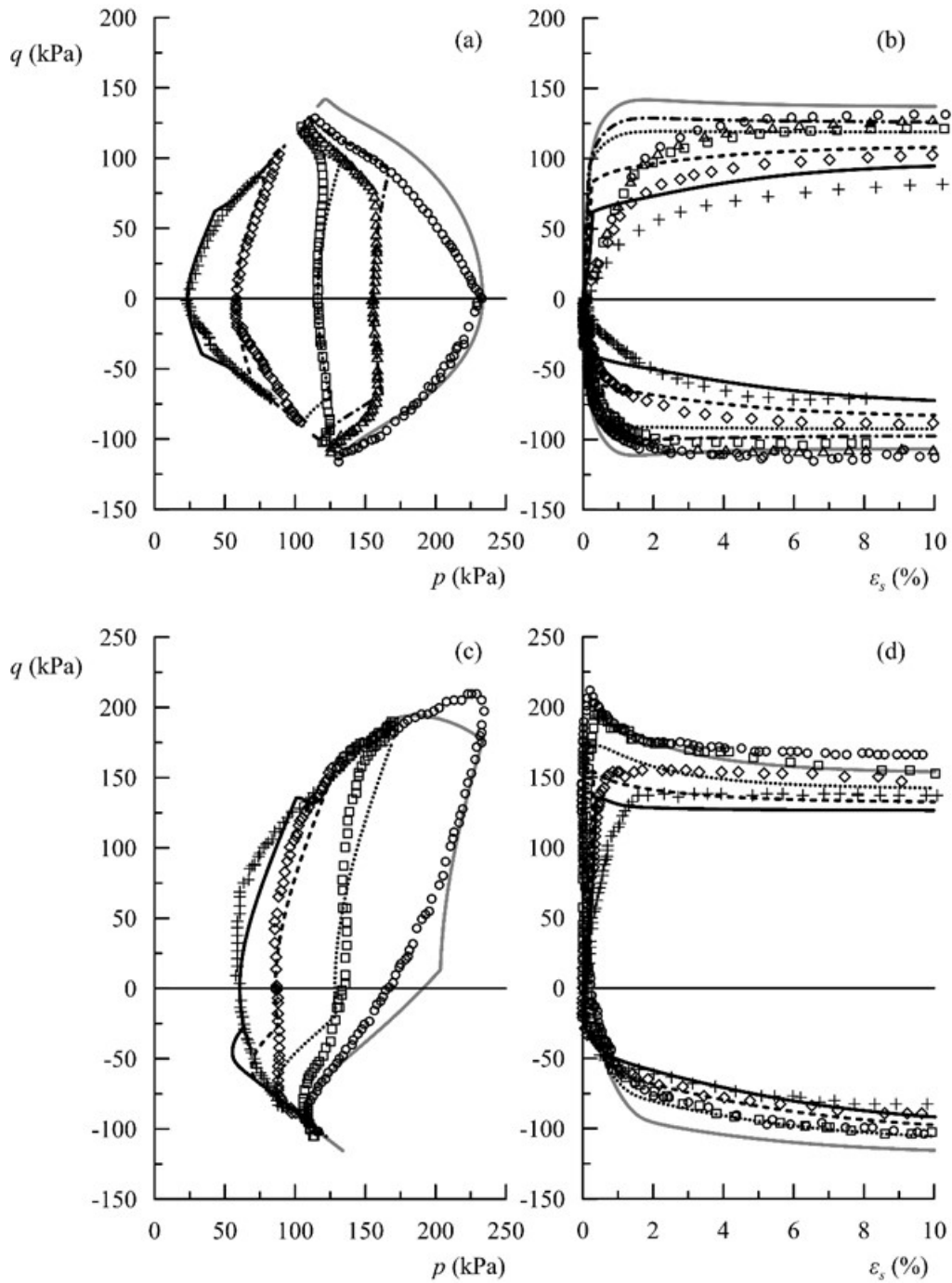
Figure 7. Comparison between data and simulations of undrained triaxial tests for isotropically consolidated (a,b) and K_0-consolidated (c,d) samples of LCT clay

Finally, Figure 8 compares the results of drained triaxial compression tests with experimental data by Gens (1982) on LCT clay for isotropic and anisotropic consolidated samples for OCR = 1, 1.5, 2, 4. The results are plotted in the $\varepsilon_a - q$ and $\varepsilon_a - \varepsilon_v$ planes, with ε_a axial strain. The stress-strain curves satisfactorily reproduce the experimental results while the model underpredicts the volumetric response.
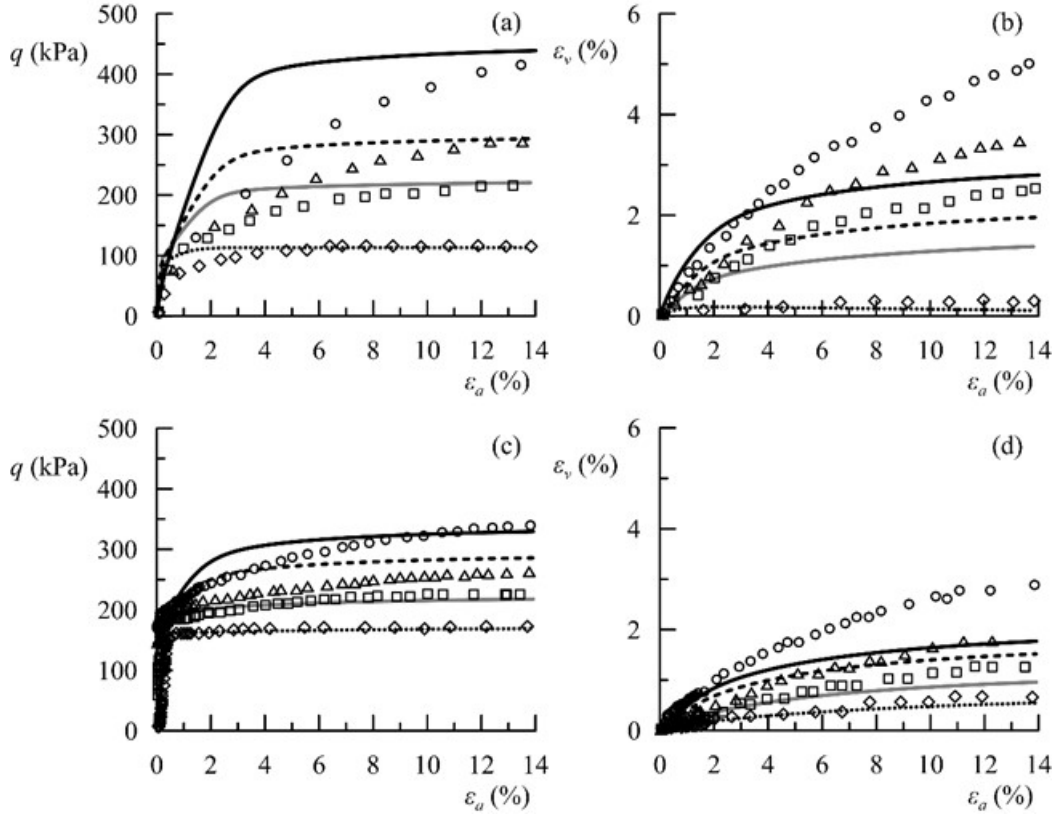
Figure 8. Comparison between data and simulations of drained triaxial tests for isotropically consolidated (a,b) and K_0-consolidated (c,d) samples of LCT clay

6 Conclusions

In this work the single surface elasto-plastic anisotropic model for clays SANICLAY modified by Dafalias & Taiebat (2013) is revisited in a thermodynamic perspective. Within the framework of hyperelasto-plasticity the model is first presented in the triaxial formulation and then generalised to the multiaxial stress-strain space. The formulation is based on two scalar potential functions, the free energy and the rate of dissipation, thus guaranteeing the thermodynamic consistency of the model. The associated version of the SANICLAY-T model coincides, for the plastic regime, with the original one developed within the framework of classical elasto-plasticity, proving its thermodynamic consistency. Subsequently, a non-associated version of the model is obtained introducing a dependence of the dissipation function on the mean effective pressure. The non-associated flow rule leads to non-elliptic yield loci in the Cauchy stress space, whereas in the generalised stress space the yield surface is always a distorted ellipse with associated flow rule. The proposed formulation results in a more flexible model, as compared to the original elasto-plastic version, as it allows for non-elliptic yield loci, which seem to be more appropriate to reproduce the behaviour of natural clays. We

26

demonstrated that, differently from most of the hyperplastic anisotropic models available in the literature, a proper combination of the free energy and the dissipation functions allows to introduce an isotropic hardening depending only on the volumetric plastic strains, as in the original elasto-plastic SANICLAY model. Furthermore, the formulation is able to reproduce the anisotropic character of clays at critical state by a permanent distortion of the yield surface. In fact, as the stored energy term is not included in the potential, the rotational variable β can assume any value at critical state in a consistent thermodynamic form. Therefore, the user is free to adopt the specific rotational hardening law which better suits the specific application.

The proposed constitutive relation, despite its relatively simple analytical formulation, proves to realistically reproduce some of the main features of the behaviour of clayey soils. The validation proposed here indicates that the non-associated version of the SANICLAY-T model should be preferred when simulating the behaviour of clays: for example, this assumption allows to mimic the fragile stress-strain curves typically observed in K_0-compressed specimens of normally consolidated, or lightly overconsolidated, clays when shared undrained under triaxial conditions. The introduction of a nonlinear isotropic hyperelastic formulations improves the predictive capability of the model within the yield surface as compared to the typical hypoelastic model adopted in the SANICLAY model, though we are aware that in that range the performance could be significantly improved by adopting a continuous hyperplastic approach (e.g. Einav & Puzrin, 2004a; Likitlersuang & Houlsby, 2006; Apriadi et al., 2013).

Appendix A

In the following a simple procedure to derive the yield function from the dissipation function for the general case of non-associated flow rule is illustrated. At this scope, the rate of the internal variables should be expressed in terms of the dissipative generalised stresses. Recalling the definition of the dissipative generalised stress, from Eq. (12) it follows:

$$\chi_p = \frac{\partial d}{\partial \dot{\alpha}_p} = \frac{A^2 \left(\dot{\alpha}_p + \beta \dot{\alpha}_q \right)}{\sqrt{A^2 \left(\dot{\alpha}_p + \beta \dot{\alpha}_q \right)^2 + B^2 \left(M^2 - \beta^2 \right) \dot{\alpha}_q^2}} + \frac{\gamma p_0}{2} \tag{A1a}$$

and

$$\chi_q = \frac{\partial d}{\partial \dot{\alpha}_q} = \frac{B^2 \left(M^2 - \beta^2 \right) \dot{\alpha}_q + A^2 \beta \left(\dot{\alpha}_p + \beta \dot{\alpha}_q \right)}{\sqrt{A^2 \left(\dot{\alpha}_p + \beta \dot{\alpha}_q \right)^2 + B^2 \left(M^2 - \beta^2 \right) \dot{\alpha}_q^2}} + \beta \frac{\gamma p_0}{2} \tag{A1b}$$

From the above equations one can deduce the rates of internal variables $\dot{\alpha}_p$ and $\dot{\alpha}_q$. In this sense, the convenient position $\bar{d} = \sqrt{A^2\left(\dot{\alpha}_p + \beta\dot{\alpha}_q\right)^2 + B^2\left(M^2 - \beta^2\right)\dot{\alpha}_q^2}$ is made, leading to:

$$\chi_p - \frac{\gamma p_0}{2} = \frac{A^2\left(\dot{\alpha}_p + \beta\dot{\alpha}_q\right)}{\bar{d}} \tag{A2a}$$

and

$$\chi_q - \beta\frac{\gamma p_0}{2} = \frac{B^2\left(M^2 - \beta^2\right)\dot{\alpha}_q + A^2\beta\left(\dot{\alpha}_p + \beta\dot{\alpha}_q\right)}{\bar{d}} \tag{A2b}$$

from which, after few calculations, the rate of the internal variables can be expressed as a function of the dissipative generalised stresses as follow:

$$\dot{\alpha}_p = \left(\chi_p - \frac{\gamma p_0}{2}\right)\frac{\bar{d}}{A^2} - \frac{\beta}{B^2\left(M^2 - \beta^2\right)}\left(\chi_q - \beta\chi_p\right)\bar{d} \tag{A3a}$$

and

$$\dot{\alpha}_q = \frac{\chi_q - \beta\chi_p}{B^2\left(M^2 - \beta^2\right)}\bar{d} \tag{A3b}$$

Now, substituting Eqs. (A3) in the expression of $\bar{d}$ and raising to the power of two, one can write:

$$\bar{d}^2 = A^2\left(\dot{\alpha}_p + \beta\dot{\alpha}_q\right)^2 + B^2\left(M^2 - \beta^2\right)\dot{\alpha}_q^2 = \left(\chi_p - \frac{\gamma p_0}{2}\right)^2\frac{\bar{d}^2}{A^2} + \frac{\left(\chi_q - \beta\chi_p\right)^2}{B^2\left(M^2 - \beta^2\right)}\bar{d}^2 \tag{A4}$$

Therefore, $\bar{d}^2$ can be eliminated from Eq. (A4) and multiplying all the members for the term $A^2 B^2\left(M^2 - \beta^2\right)$ results in:

$$A^2\left(\chi_q - \beta\chi_p\right)^2 + B^2\left(M^2 - \beta^2\right)\left(\chi_p - \frac{\gamma p_0}{2}\right)^2 - A^2 B^2\left(M^2 - \beta^2\right) = 0 \tag{A5}$$

that is the equation of the yield function in the dissipative generalised stress plane of Eq. (14).

Appendix B

As for classical elastoplasticity, the consistency condition can be imposed to obtain the plastic multiplier and express the constitutive relationship in its incremental form. For the proposed model, under the simplified triaxial conditions explored in the validation Section 5, it is:

$$\dot{f} = \frac{\partial f}{\partial \chi_p}\dot{\chi}_p + \frac{\partial f}{\partial \chi_q}\dot{\chi}_q + \frac{\partial f}{\partial p}\dot{p} + \frac{\partial f}{\partial \beta}\dot{\beta} + \frac{\partial f}{\partial p_0}\dot{p}_0 =$$

$$= \frac{\partial f}{\partial \chi_p}\dot{\chi}_p + \frac{\partial f}{\partial \chi_q}\dot{\chi}_q + \frac{\partial f}{\partial p}\dot{p} + \frac{\partial f}{\partial \beta}\langle L\rangle cp(\beta_b - \beta) + \frac{\partial f}{\partial p_0}\frac{\partial p_0}{\partial \alpha_p}\langle L\rangle\frac{\partial f}{\partial \chi_p} = 0 \tag{B1}$$

where the rate of the internal variables p_0 and β are expressed by the isotropic and rotational hardening rules reported in Eqs. (7) and (8), respectively. From eq. (B1) the plastic multiplier can be specified:

$$L = \frac{\dfrac{\partial f}{\partial \chi_p}\dot{\chi}_p + \dfrac{\partial f}{\partial \chi_q}\dot{\chi}_q + \dfrac{\partial f}{\partial p}\dot{p}}{\dfrac{\partial f}{\partial \beta}cp(\beta_b - \beta) + \dfrac{\partial f}{\partial p_0}\dfrac{\partial p_0}{\partial \alpha_p}\dfrac{\partial f}{\partial \chi_p}} \tag{B2}$$

To guarantee that all the derivatives entering in Eq. (B2) are dimensionally consistent, the yield function in Eq. (14) is divided by the term A^2. The directions of the plastic flow are:

$$\frac{\partial f}{\partial \chi_p} = -2\beta\left(\chi_q - \beta\chi_p\right) + 2\left(M^2 - \beta^2\right)\frac{B^2}{A^2}\left(\chi_p - \frac{\gamma p_0}{2}\right) \tag{B3}$$

and

$$\frac{\partial f}{\partial \chi_q} = 2\chi_q - 2\beta\chi_p \tag{B4}$$

Note that in this case the direction of plastic strain rates depends on the parameters γ and δ as well as on the mean effective pressure via the quantities A and B. The other useful derivatives are:

$$\frac{\partial f}{\partial \beta} = \frac{\partial \hat{f}}{\partial \beta} = -2\chi_p\left(\chi_q - \beta\chi_p\right) - 2\beta\frac{B^2}{A^2}\left(\chi_p - \frac{\gamma p_0}{2}\right)^2 + 2\beta B^2 \tag{B5}$$

$$\frac{\partial p_0}{\partial \alpha_p} = \frac{1 + e_{in}}{\lambda - \kappa}p_0 \tag{B6}$$

$$\frac{\partial f}{\partial p_0} = \frac{\partial \hat{f}}{\partial p_0} = -\left(M^2 - \beta^2\right)\frac{B^2}{A^2}\gamma\left(\chi_p - \frac{\gamma p_0}{2}\right) - 2B\left(M^2 - \beta^2\right)\frac{\partial B}{\partial p_0} +$$

$$+ \left(M^2 - \beta^2\right)\left(\chi_p - \frac{\gamma p_0}{2}\right)^2\frac{2BA^2\dfrac{\partial B}{\partial p_0} - 2AB^2\dfrac{\partial A}{\partial p_0}}{A^4} \tag{B7}$$

with

$$\frac{\partial A}{\partial p_0} = \frac{\gamma}{2}; \quad \frac{\partial B}{\partial p_0} = \frac{\gamma\delta}{2} \tag{B8}$$

and

$$\frac{\partial f}{\partial p} = \left(M^2 - \beta^2\right)\left(\chi_p - \frac{\gamma p_0}{2}\right)^2 \frac{2BA^2 \frac{\partial B}{\partial p} - 2AB^2 \frac{\partial A}{\partial p}}{A^4} - 2B\left(M^2 - \beta^2\right)\frac{\partial B}{\partial p} \tag{B9}$$

with

$$\frac{\partial A}{\partial p} = 1 - \gamma; \quad \frac{\partial B}{\partial p} = 1 - \delta \tag{B10}$$

Finally, the derivatives of the yield function $\hat{f}$ with respect to the stress are:

$$\frac{\partial \hat{f}}{\partial p} = -2\beta\left(q - \beta p\right) + 2\left(M^2 - \beta^2\right)\frac{B^2}{A^2}\left(p - \frac{\gamma p_0}{2}\right) +$$

$$+ \left(M^2 - \beta^2\right)\left(\chi_p - \frac{\gamma p_0}{2}\right)^2 \frac{2BA^2 \frac{\partial B}{\partial p} - 2AB^2 \frac{\partial A}{\partial p}}{A^4} - 2B\left(M^2 - \beta^2\right)\frac{\partial B}{\partial p} \tag{B11}$$

and

$$\frac{\partial \hat{f}}{\partial q} = 2q - 2\beta p \tag{B12}$$

Notation

A, B	Terms of the dissipation function in Eq. (12)
c	RH parameter for Eq. (8)
$\dot{d}$	Rate of dissipation
D_{ijkl}	Stiffness tensor
e	Void ratio
e_{in}	Initial void ratio
f	Yield function in generalised stress space
$\hat{f}$	Yield function in stress space
g	Dimensionless shear modulus coefficient
H	Hardening modulus
k	Dimensionless bulk modulus coefficient
L	Plastic multiplier
M	Critical stress ratio
m	RH parameter of Eq. (9)
n	Exponent in power-law relationship for elastic stiffness
$n*$	RH parameter of Eq. (9)
N	Peak stress ratio on the yield surface for the Dafalias & Taiebat (2013) model
p	Mean effective stress
p_0	Size of the yield surface along the p-axis
$p_{0,in}$	Initial size of the yield surface along the p-axis
p_r	Reference pressure
q	Deviatoric stress
r_{ij}	Stress ratio tensor
v	Specific volume
x	RH parameter
α_{ij}	Internal variable tensor
α_p, α_q	Internal variable in p-q plane
β_{ij}	Rotational hardening variable
$\beta_{b,ij}$	Bound of β_{ij}
β	Rotational hardening variable in p-q plane
β_b	Bound of β in p-q plane
β_c	RH parameter of Eq. (9)
γ	Parameter for the non-associated model
δ	Parameter for the non-associated model
δ_{ij}	Kronecker delta
ε_{ij}	Strain tensor
ε'_{ij}	Deviatoric part of the strain tensor
ε_s	Deviatoric strain invariant
ε_v	Volumetric strain

η	Stress ratio
κ	Slope of the rebound line in $e - \ln p$ plane
$\tilde{\kappa}$	Slope of the rebound line in $\ln v - \ln p$ plane
λ	Slope of the compression line in $e - \ln p$ plane
$\tilde{\lambda}$	Slope of the compression line in $\ln v - \ln p$ plane
μ	RH parameter
v	Poisson's ratio
σ_{ij}	Stress tensor
σ'_{ij}	Deviatoric part of the stress tensor
φ	Helmholtz free energy
$\overline{\chi}_{ij}$	Generalised stress tensor
$\overline{\chi}_p, \overline{\chi}_q$	Generalised stresses in triaxial formulation
χ_{ij}	Dissipative generalised stress tensor
χ'_{ij}	Deviatoric part of dissipative generalised stress tensor
χ_p, χ_q	Dissipative generalised stresses in triaxial formulation
ψ, ψ_1, ψ_2	Gibbs free energy

References

Al-Sharrad, M. A., Gallipoli, D., & Wheeler, S. J. (2017). Experimental investigation of evolving anisotropy in unsaturated soils. *Géotechnique*, *67*(12), 1033-1049.

Amorosi, A., Rollo, F., & Houlsby, G. T. (2020). A nonlinear anisotropic hyperelastic formulation for granular materials: comparison with existing models and validation. *Acta Geotechnica*, *15*(1), 179-196.

Apriadi, D., Likitlersuang, S., & Pipatpongsa, T. (2013). Loading path dependence and non-linear stiffness at small strain using rate-dependent multisurface hyperplasticity model. *Computers and Geotechnics*, *49*, 100-110.

Callisto, L., & Calabresi, G. (1998). Mechanical behaviour of a natural soft clay. *Géotechnique*, *48*(4), 495-513.

Chen, Y., & Yang, Z. (2019). A bounding surface model for anisotropically overconsolidated clay incorporating thermodynamics admissible rotational hardening rule. *International Journal for Numerical and Analytical Methods in Geomechanics*, 1-23. https://doi.org/10.1002/nag.3032.

Chin, C. T., Chen, J. R., Hu, I. C., Yao, D., & Chao, H. C. (2007). Engineering characteristics of Taipei clay. In *Proceedings of the 2nd International Workshop on Characterization and Engineering Properties of Natural Soils, Singapore* (Vol. 29, pp. 1755-1804). London, UK: Taylor & Francis.

Collins, I. F. (2003). A systematic procedure for constructing critical state models in three dimensions. *International Journal of Solids and Structures*, *40*(17), 4379-4397.

Collins, I. F. (2005). Elastic/plastic models for soils and sands. *International Journal of Mechanical Sciences*, *47*(4-5), 493-508.

Collins, I. F., & Hilder, T. (2002). A theoretical framework for constructing elastic/plastic constitutive models of triaxial tests. *International Journal for Numerical and Analytical Methods in Geomechanics*, *26*(13), 1313-1347.

Collins, I. F., & Houlsby, G. T. (1997). Application of thermomechanical principles to the modelling of geotechnical materials. *Proc. of the Royal Society of London A: Mathematical, physical and engineering sciences* (Vol. 453, No. 1964, pp. 1975-2001).

Collins, I. F., & Kelly, P. A. (2002). A thermomechanical analysis of a family of soil models. *Geotechnique*, *52*(7), 507-518.

Coombs, W. M. (2011). Finite deformation of particulate geomaterials: frictional and anisotropic Critical State elasto-plasticity. PhD Thesis, Durham University.

Coombs, W. M., & Crouch, R. S. (2011). Algorithmic issues for three-invariant hyperplastic Critical State models. *Computer Methods in Applied Mechanics and Engineering*, *200*(25-28), 2297-2318.

Coombs, W. M., Crouch, R. S., & Augarde, C. E. (2013). A unique critical state two-surface hyperplasticity model for fine-grained particulate media. *Journal of the Mechanics and Physics of Solids*, *61*(1), 175-189.

Coombs, W. M. (2017). Continuously unique anisotropic critical state hyperplasticity. *International Journal for Numerical and Analytical Methods in Geomechanics*, *41*(4), 578-601.

Cudny, M., & Partyka, E. (2017). Influence of anisotropic stiffness in numerical analyses of tunneling and excavation problems in stiff soils. In *Proceedings of the 19th international conference on soil mechanics and geotechnical engineering, Seoul* (pp. 719-722).

Dafalias, Y. F. (1986). An anisotropic critical state soil plasticity model. *Mechanics Research Communications*, *13*(6), 341-347.

Dafalias, Y. F., Manzari, M. T., & Papadimitriou, A. G. (2006). SANICLAY: simple anisotropic clay plasticity model. *International Journal for Numerical and Analytical Methods in Geomechanics*, *30*(12), 1231-1257.

Dafalias, Y. F., & Taiebat, M. (2013). Anatomy of rotational hardening in clay plasticity. *Géotechnique*, *63*(16), 1406-1418.

Dafalias, Y. F., & Taiebat, M. (2014). Rotational hardening with and without anisotropic fabric at critical state. *Géotechnique*, *64*(6), 507-511.

Dafalias, Y. F., Rollo, F., Amorosi, A., Taiebat, M. (2020). Convergence of rotational hardening with bounds in clay plasticity. *10*(1), 1-4 https://doi.org/10.1680/jgele.19.00012.

Diaz-Rodriguez, J. A., Leroueil, S., & Aleman, J. D. (1992). Yielding of Mexico City clay and other natural clays. *Journal of geotechnical engineering*, *118*(7), 981-995.

Einav, I., & Puzrin, A. M. (2004a). Continuous hyperplastic critical state (CHCS) model: derivation. *International journal of solids and structures*, *41*(1), 199-226.

Einav, I., & Puzrin, A. M. (2004b). Pressure-dependent elasticity and energy conservation in elastoplastic models for soils. *Journal of Geotechnical and Geoenvironmental Engineering*, *130*(1), 81-92.

Fu, P., & Dafalias, Y. F. (2011). Fabric evolution within shear bands of granular materials and its relation to critical state theory. *International Journal for numerical and analytical methods in geomechanics*, *35*(18), 1918-1948.

Franzius, J. N., Potts, D. M., & Burland, J. B. (2005). The influence of soil anisotropy and K 0 on ground surface movements resulting from tunnel excavation. *Géotechnique*, *55*(3), 189-199.

Gens, A. (1982). Stress-strain and strength characteristics of a low plasticity clay. PhD Thesis, Imperial College, London.

Guo, N., & Zhao, J. (2013). The signature of shear-induced anisotropy in granular media. *Computers and Geotechnics*, *47*, 1-15.

Halphen, B., Nguyen, Quoc Son. (1975). Sur les matériaux standards généralisés. *J. Méc*. 14, 39–63.

Hashiguchi, K. (1977). An expression of anisotropy in a plastic constitutive equation of soils. S. Murayama and A. N. Schofield (eds), *Constitutive Equations of Soils, Proc. 9th Int. Conf. Soil Mech. Found. Eng., Spec. Session 9, JSSMFE*, Tokyo, pp. 302-305.

Houlsby, G.T. (2019). Hyperplasticity - An approach to plasticity theory based on thermodynamics. https://hyperplasticity.wordpress.com*/*.

Houlsby, G.T., Amorosi, A., & Rojas, E. (2005). Elastic moduli of soils dependent on pressure: a hyperelastic formulation. *Géotechnique* **55** (5), 383-392.

Houlsby, G. T., Amorosi, A., & Rollo, F. (2019). Non-linear anisotropic hyperelasticity for granular materials. *Computers and Geotechnics* **115**, 103167.

Houlsby, G. T., & Puzrin, A. M. (2000). A thermomechanical framework for constitutive models for rate-independent dissipative materials. *International journal of Plasticity*, *16*(9), 1017-1047.

Houlsby, G. T., & Puzrin, A. M. (2006). *Principles of hyperplasticity.* Springer - Verlag London Limited.

Huang, M., Liu, Y., & Sheng, D. (2011). Simulation of yielding and stress–stain behavior of shanghai soft clay. *Computers and Geotechnics*, *38*(3), 341-353.

Jiang, J., & Ling, H. (2010). A framework of an anisotropic elastoplastic model for clays. *Mech. Res. Comm. 37(4),* 394-398.

Karstunen, M., Krenn, H., Wheeler, S. J., Koskinen, M., & Zentar, R. (2005). Effect of anisotropy and destructuration on the behavior of Murro test embankment. *International Journal of Geomechanics*, *5*(2), 87-97.

Kim, T., & Finno, R. J. (2012). Anisotropy evolution and irrecoverable deformation in triaxial stress probes. *Journal of Geotechnical and Geoenvironmental Engineering*, *138*(2), 155-165.

Ko, H. Y., & Masson, R. M. (1976). Nonlinear characterization and analysis of sand. In *2nd Int. Conf. on Numerical Methods in Geomechanics*. ASCE, Blacksburg, Va, pp. 294-305.

Likitlersuang, S., & Houlsby, G. T. (2006). Development of hyperplasticity models for soil mechanics. *International journal for numerical and analytical methods in geomechanics*, *30*(3), 229-254.

Liu, W., Shi, M., Miao, L., Xu, L., & Zhang, D. (2013). Constitutive modeling of the destructuration and anisotropy of natural soft clay. *Computers and Geotechnics*, *51*, 24-41.

Masson, S., & Martinez, J. (2001). Micromechanical analysis of the shear behavior of a granular material. *Journal of engineering mechanics*, *127*(10), 1007-1016.

Maugin, G. A. (1992). *The thermomechanics of plasticity and fracture*. Cambridge University Press, Cambridge.

Puzrin, A. M., Burland, J. B., & Standing, J. R. (2012). Simple approach to predicting ground displacements caused by tunnelling in undrained anisotropic elastic soil. *Géotechnique*, *62*(4), 341-352.

Rezania, M., Mousavi Nezhad, M., Zanganeh, H., Castro, J., & Sivasithamparam, N. (2017). Modeling pile setup in natural clay deposit considering soil anisotropy, structure, and creep effects: Case study. *International Journal of Geomechanics*, *17*(3), 04016075.

Rezania, M., Nguyen, H., Zanganeh, H., & Taiebat, M. (2018). Numerical analysis of Ballina test embankment on a soft structured clay foundation. *Computers and Geotechnics*, *93*, 61-74.

Sekiguchi, H. & Ohta, K. (1977). Induced anisotropy and time dependence in clays. *Proceedings of the 9th International Conference on Soil Mechanics and Foundation Engineering (Specialty Session 9)*, Tokyo, Japan, pp. 229–238.

Simpson, B., Atkinson, J. H., & Jovičić, V. (1996). The Influence of Anisotropy on Calculations of Ground Settlements Above Tunnels. *Proceedings, Geotechnical Aspects of Underground Construction in Soft Ground*, Balkema, Rotterdam, pp. 591-595.

Simpson, B. (2017). Anisotropic linear elastic materials subject to undrained plane strain deformation. *Géotechnique*, *67*(8), 728-732.

Sivasithamparam, N., & Castro, J. (2016). An anisotropic elastoplastic model for soft clays based on logarithmic contractancy. *International Journal for Numerical and Analytical Methods in Geomechanics*, *40*(4), 596-621.

Sivasithamparam, N., & Rezania, M. (2017). The comparison of modelling inherent and evolving anisotropy on the behaviour of a full-scale embankment. *International Journal of Geotechnical Engineering*, *11*(4), 343-354.

Smith, P. R., Jardine, R. J., & Hight, D. W. (1992). The yielding of Bothkennar clay. *Géotechnique*, *42*(2), 257-274.

Theocharis, A. I., Vairaktaris, E., Dafalias, Y. F., & Papadimitriou, A. G. (2019). Necessary and sufficient conditions for reaching and maintaining critical state. *International Journal for Numerical and Analytical Methods in Geomechanics*, *43*(12), 2041-2055.

Wang, R., Fu, P., Zhang, J. M., & Dafalias, Y. F. (2017). Evolution of various fabric tensors for granular media toward the critical state. *Journal of Engineering Mechanics*, *143*(10), 04017117.

Wang, R., Dafalias, Y. F., Fu, P., & Zhang, J. M. (2020). Fabric evolution and dilatancy within anisotropic critical state theory guided and validated by DEM. *International Journal of Solids and Structures*, *188*, 210-222.

Wheeler, S. J., Näätänen, A., Karstunen, M., & Lojander, M. (2003). An anisotropic elastoplastic model for soft clays. *Canadian Geotechnical Journal*, *40*(2), 403-418.

Whittle, A. J., & Kavvadas, M. J. (1994). Formulation of MIT-E3 constitutive model for overconsolidated clays. *Journal of Geotechnical Engineering*, *120*(1), 173-198.

Yang, C., Carter, J. P., & Yu, S. (2015). Comparison of model predictions of the anisotropic plasticity of Lower Cromer Till. *Computers and Geotechnics*, *69*, 365-377.

Yang, Z. X., & Wu, Y. (2017). Critical state for anisotropic granular materials: a discrete element perspective. *International Journal of Geomechanics*, *17*(2), 04016054.

Zdravković, L., Potts, D. M., & Hight, D. W. (2002). The effect of strength anisotropy on the behaviour of embankments on soft ground. *Géotechnique*, *52*(6), 447-457.

Zhang, H., Chen, Q., Chen, J., & Wang, J. (2016). Unified Expression of Rotational Hardening in Clay Plasticity. *International Journal of Geomechanics*, *16*(6), 06016004-1 - 06016004-8.

Zhang, Z., Chen, Y., & Huang, Z. (2018). A novel constitutive model for geomaterials in hyperplasticity. *Computers and Geotechnics*, *98*, 102-113.

Ziegler, H. (1977). An introduction to thermomechanics, North Holland, Amsterdam.

Zymnis, D. M., Chatzigiannelis, I., & Whittle, A. J. (2013). Effect of anisotropy in ground movements caused by tunnelling. *Géotechnique*, *63*(13), 1083-1102.

Zytynski, M., Randolph, M. F., Nova, R., & Wroth, C. P. (1978). On modelling the unloading-reloading behaviour of soils. *International Journal for Numerical and Analytical Methods in Geomechanics*, *2*(1), 87-93.